

Study on phase error of binary fringe from defocusing projection

QIAO Nao-sheng, CAO Bin-fang

Citation:

QIAO Nao-sheng, CAO Bin-fang. Study on phase error of binary fringe from defocusing projection[J]. *Chinese Optics*, In press. doi: 10.37188/CO.EN-2025-0046

乔闹生, 曹斌芳. 二值条纹离焦投影的相位误差研究[J]. *中国光学*, 优先发表. doi: 10.37188/CO.EN-2025-0046

View online: <https://doi.org/10.37188/CO.EN-2025-0046>

Articles you may be interested in

[Phase measurement with dual-frequency grating in a nonlinear system](#)

非线性系统中双频光栅相位测量

Chinese Optics. 2023, 16(3): 726 <https://doi.org/10.37188/CO.EN.2022-0013>

[Dynamic 3D measurement error compensation technology based on phase-shifting and fringe projection](#)

基于相移条纹投影的动态3D测量误差补偿技术

Chinese Optics. 2023, 16(1): 184 <https://doi.org/10.37188/CO.EN.2022-0004>

[Nonlinear error active coding optimal estimation correction method for fringe projection](#)

条纹投影非线性误差主动编码最优估计校正方法

Chinese Optics. 2025, 18(6): 1365 <https://doi.org/10.37188/CO.2024-0167>

[Phase measurement technique based on MHz-lever depth frequency modulated laser interferometry](#)

基于MHz深度频率调制激光干涉的相位测量技术

Chinese Optics. 2025, 18(3): 622 <https://doi.org/10.37188/CO.2024-0157>

[Optimal fringe frequency allocation for non-standard phase-shifting profilometry](#)

非标准相移轮廓术的最优条纹频率分配

Chinese Optics. 2025, 18(2): 245 <https://doi.org/10.37188/CO.2024-0163>

[Error correction of complex texture objects based on bidirectional fringe projection point cloud matching](#)

基于双向条纹点云匹配的复杂纹理误差校正

Chinese Optics. 2025, 18(5): 1086 <https://doi.org/10.37188/CO.2025-0040>

Study on phase error of binary fringe from defocusing projection

QIAO Nao-sheng^{1,2*}, CAO Bin-fang²

(1. *International College, Hunan University of Arts and Science, Changde 415000, P.R.China;*
2. *Hunan Provincial Key Laboratory of Distributed Electric Propulsion Vehicle Control Technology,*
Changde 415000, P.R.China)

* *Corresponding author, E-mail: naoshengqiao@163.com*

Abstract: Due to the nonlinear effects produced by the actual defocusing projection system, which affect the accuracy of phase measurement, the phase error of binary fringe defocusing projection was studied. Based on the analysis of the current study status in the field, an expression for the intensity distribution of deformed fringe pattern signal in nonlinear systems is given, and the reasons for both high-order spectra components occurrence and their mixing with the fundamental frequency components, resulting in spectra overlapping, are analyzed. The method of defocusing the projector was employed to remove the higher-order harmonic components in the spectra domain and filter out one of the fundamental frequency components. An inverse Fourier transform was then performed on the spectra to obtain the expression of fringe intensity in the spatial domain. The continuous phase containing continuous signals was obtained using the phase-shift algorithm and phase unwrapping, and the expression for phase error after unwrapping in actual measurement systems was derived. The correct analysis of the basic principles has been verified through simulation and experiments. The simulation results indicate that the errors value obtained by the method mentioned in this paper are 34.51% for the binary fringe defocusing method, 44.83% for method of reference [1], and 67.83% for method of reference [10], respectively. The experiment results indicate that the phase recovered by using our method has good effects, and the corresponding phase error is relatively small.

Key words: phase measurement; defocusing projection; system nonlinear; phase-shifting; phase error

收稿日期:2025-12-18; 修订日期:xxxx-xx-xx

基金项目:湖南省教育厅科学研究重点项目(No. 22A0484); 湖南省自然科学基金项目(No. 2026JJ80289); 国家自然科学基金(No. 62573191)

Supported by Key Scientific Research Project of Hunan Provincial Department of Education (No. 22A0484); Hunan Provincial Natural Science Foundation of China (No. 2026JJ80289); National Natural Science Foundation of China (No. 62573191)

二值条纹离焦投影的相位误差研究

乔闹生^{1,2*}, 曹斌芳²

(1. 湖南文理学院 国际学院, 湖南 常德 415000;

2. 分布式电推进飞行器控制技术湖南省重点实验室, 湖南 常德 415000)

摘要: 由于实际的离焦投影系统产生非线性效应, 影响了相位测量精度, 为此对二值条纹离焦投影的相位误差展开研究。基于该领域研究现状分析, 给出了非线性系统中变形条纹图信号光强的分布表达式, 分析了频谱中出现了高级频谱成份并与基频成份混在一起产生混叠现象的原因。采用了对投影仪进行离焦处理的方法滤除频谱中的高级频谱成份, 过滤出其中的一个基频成份并进行逆傅里叶变换, 得到空间域中的条纹光强表达式; 采用相移算法与相位展开得到包含连续信号的连续相位, 推导出了在实际测量中进行相位展开后的误差表达式。用仿真与实验验证了基本原理的正确分析, 仿真结果表明, 采用本文方法所得误差值分别为二值条纹离焦法的 34.51%、参考文献 [1] 的 44.83%、参考文献 [10] 的 67.83%; 实验结果表明, 采用本文方法具有良好的相位恢复效果, 且相对应的相位误差也比较小。

关键词: 相位测量; 离焦投影; 系统非线性; 相移; 相位误差

中图分类号: O438.2

文献标志码: A

doi: 10.37188/CO.EN-2025-0046

CSTR: 32171.14.CO.EN-2025-0046

1 Introduction

Phase measurement profilometry is a highly important research topic in optical three-dimensional shape measurement. It is widely used in various fields due to its high accuracy, good stability, and ease of implementation in engineering application^[1-3]. However, due to uneven illumination during the measurement process or the influence of external factors, the actual measurement system is a defocusing nonlinear system, which produces nonlinear gamma effects and affects phase measurement. Many scholars around the world have conducted in-depth research on these problems^[4-14]. For example, Wang *et al.* proposed a high-precision active projection phase measurement error correction method, which is easy to implement and insensitive to projector defocusing. This method thereby reduce the impact of brightness nonlinear caused by the superimposed gamma effect from the projector or camera, and increase measurement accuracy and resolution^[4]. Yang *et al.* proposed that standard Gaussian fringes can be displayed in both directions of a liquid crystal display when studying phase-shifting modes. When affected by nonlinear or image defo-

cusing of the liquid crystal display, standard Gaussian fringes can still accurately extract feature points, thereby improving the accuracy of feature point extraction and camera calibration^[5]. In 2025, Zhang *et al.* proposed a complex texture error correction method based on bidirectional fringe point cloud matching in a structured light three-dimensional measurement system. This method accurately reconstructed the phase of objects with complex textures, reduced the phase error introduced by complex textures on the object surface under camera defocusing conditions, and improved its measurement accuracy^[6].

In the process of phase measurement, phase errors are inevitably generated due to the nonlinear effects of the system. Therefore, some scholars worldwide have conducted extensive research on reducing phase errors and have achieved some better research results^[8-14]. For example, In 2020, Liu Y *et al.* proposed a fast phase error compensation technique based on package phase distribution, which reduced the nonlinear effects in phase measurement and achieved fast and simple phase error compensation^[8]. In 2023, based on fitting the double response curve, Wang J *et al.* proposed a fast active gamma compensation method, which reduced the

nonlinear phase error caused by the nonlinear gamma effect of projector or camera in fringe projection systems^[9]. In 2024, Zhang W *et al.* proposed a method of fusing two wrapped phases to correct phase errors, thereby reducing phase errors caused by the nonlinear responses of projectors and cameras in phase measurements^[10].

To solve the error problem of phase measurement in nonlinear systems for defocusing projection, this paper investigates the generation and reduction methods of phase measurement errors in binary fringe defocusing projection systems, aiming to minimize spectra overlapping caused by system defocusing nonlinear as much as possible. The Gaussian function filtering method, phase-shifting method, and polynomial expansion method are used to effectively reduce phase errors caused by gamma nonlinear effects in defocusing projection systems, and it can calculate the value of these errors. The accuracy and rationality of the basic principle analysis are verified through computer simulation and actual experiments. The results indicate that the error values obtained using our method are smaller than those of the binary fringe defocusing method, the method of reference [1], and the method of reference [10].

2 Principle analysis

When the Rochesteer grating is projected onto the surface of a diffuse reflection measured object, there exists a linear relationship between the two-dimensional deformed fringe pattern signal acquired by a ideal Charge Coupled Device (CCD) imaging system using phase modulation and the signal output by the projector. After performing Fourier transform on the deformed fringe pattern signal and employing the π phase-shifting technique^[1], then in the frequency domain, the zero-order spectra components can be eliminated, the resulting spectra contain only the fundamental frequency component, which represents the height information of the object.

However, due to uneven lighting and other external factors, the Digital Light Projector (DLP) pro-

jection system used in actual measurements is a defocusing nonlinear system, which is affected by the nonlinear gamma effect. The expression form of the light intensity grayscale value distribution of the deformed fringe pattern signal obtained is

$$g'(x, y) = ag(x, y)^\gamma + b = \sum_{k=0}^{+\infty} A_k r(x, y) \exp\{j[2k\pi f_0 x + k\phi(x, y)]\} \quad , \quad (1)$$

where a and b are linearity coefficients, $g(x, y)$ represents the light intensity signal of the deformed fringe pattern obtained under ideal conditions, γ represents the gamma coefficient of the projector, A_k represents the Fourier coefficient from the k -th harmonic component of $g'(x, y)$, $r(x, y)$ represents the surface reflectance distribution function of the object, f_0 is the fundamental frequency of the grating, $\phi(x, y)$ is the phase information containing the height variation of the object surface.

By performing Fourier transform on Eq. (1) and using the phase-shifting technique [1], then in the frequency domain, the components of zero-order spectra are eliminated, the expression of frequency domain in light intensity is obtained as follows

$$G'(f_x, f_y) = \sum_{k=1}^{\infty} Q_k(f_x - kf_0, f_y - kf_0) + \sum_{k=1}^{\infty} Q_k^*(f_x + kf_0, f_y + kf_0) \quad , \quad (2)$$

where Q and Q^* represent the spectra and its conjugate spectra, respectively.

It can be observed that in defocusing nonlinear systems, the higher-order spectra components appear in the Fourier transformed spectra of the deformed fringes, which mix with the fundamental frequency components, causing spectra overlapping and affecting the measurement accuracy of phase.

To remove high-order harmonic components from the spectra, the projector needs to be defocused. The output signal of the defocused digital projector is a point spread function expressed as a Gaussian function, as shown in Eq. (3).

$$h(x,y) = \frac{1}{2\pi\sigma^2} \exp\left(-\frac{x^2+y^2}{2\sigma^2}\right), \quad (3)$$

where σ represents the standard deviation of the Gaussian function.

Performing Fourier transform on Eq. (3), then the Gaussian function expression in the frequency domain is obtained as

$$H(f_x, f_y) = \exp\left[\left(-\frac{1}{2}f_x^2 + f_y^2\right)\sigma^2\right], \quad (4)$$

It is obvious that the defocusing optical system functions is a low-pass filter, which can be used to filter out high-order frequency components in the spectra, retaining only one of the fundamental frequency components.

The signal defocused by the projector is input by CCD, and the frequency domain fringes of the input signal are binary fringes, the expression of their light intensity is

$$G''(f_x, f_y) = G'(f_x, f_y)H(f_x, f_y), \quad (5)$$

Performing the inverse Fourier transform on Eq. (5), and the light intensity expression of binary fringes in the spatial domain can be obtained as follows

$$g''(x,y) = F^{-1}[G''(f_x, f_y)] = F^{-1}[G'(f_x, f_y)H(f_x, f_y)] = A_1 r(x,y) \exp\{j[2\pi f_0 x + \phi(x,y) + 2n(x,y)\pi/N]\}, \quad (6)$$

where $n(x,y)$ is the grating level at point (x,y) in the fringes, which is the number of steps in phase-shifting and is an integer. N is the total steps number in the phase-shifting.

To obtain the phase $\phi(x,y)$ in Eq. (6), it can be extracted using the method of N-step phase-shifting with arctangent calculation, and the calculation formula is as follows

$$\phi(x,y) = -\arctan \left[\frac{\sum_{n=1}^N g''(x,y) \sin(2n(x,y)\pi/N)}{\sum_{n=1}^N g''(x,y) \cos(2n(x,y)\pi/N)} \right], \quad (7)$$

Due to the arctangent calculation in Eq. (7), the

obtained phase $\phi(x,y)$ is actually a wrapped phase, which is wrapped within $[-\pi, \pi]$ and requires phase unwrapping to obtain a continuous phase $\varphi(x,y)$ containing continuous signal. The expression for the relationship between $\phi(x,y)$ and $\varphi(x,y)$ is

$$\varphi(x,y) = \phi(x,y) + 2n(x,y)\pi, \quad (8)$$

Assuming that the continuous phase of $g(x,y)$ in an ideal system after transformation is $\varphi^{idea}(x,y)$, the phase error of its unwrapped phase in the actual measurement system is^[15]

$$\varepsilon(x,y) = \varphi(x,y) - \varphi^{idea}(x,y) \approx \sum_{m=1}^{m'} \xi_m \sin[mN\varphi(x,y)], \quad (9)$$

where ξ_m represents the harmonic amplitude, and $m' = \text{int}[(M+1)/N]$, where M is a polynomial order and int is used to obtain an integer symbol.

Now project the i fringe patterns with the same $n(x,y)$ and modulation degree at frequency f_i . Due to $\varphi_i = 2\pi f_i$, the phase error of Eq. (9) can be changed to as follow

$$\varepsilon_i(x,y) = \varphi_i(x,y) - \varphi_i^{idea}(x,y) \approx \sum_{m=1}^{m'} \xi_{mi} \sin[(f_i/f_1)mN\varphi_1(x,y)] \quad (10)$$

where $\varphi_i^{idea}(x,y)$ is the ideal absolute phase of the i -th pixel.

Because ξ_{mi} in Eq. (10) decreases rapidly with increasing order, only the first a few terms can be retained. By taking $i=1$ and $i=2$, φ_1 and the unknown ξ_{mi} for each pixel can be obtained. Therefore, the phase error $\varepsilon_i(x,y)$ for each pixel can be obtained from Eq. (10).

3 Computer Simulation and experiment

The proposed fundamental principles have been verified through computer simulations and actual experiments.

3.1 Computer Simulation

Firstly, computer simulation is used to verify

the effectiveness and correctness of the basic principles analysis mentioned in this paper. The Fig. 1 in reference [1] is used as the system measurement

schematic, and the system geometric parameters are set as $L/d = 4$.

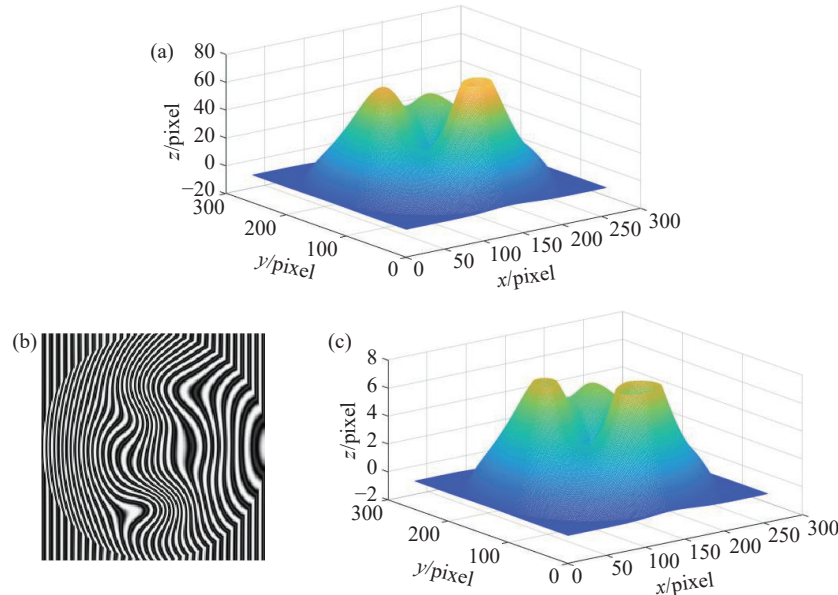


Fig. 1 Results of simulation

The object to be simulated is a three-dimensional surface diagram as shown in Fig. 1(a), with a size of 256×256 pixels. The deformation fringe pattern of the simulated object is shown in Fig. 1(b). The three-step phase-shifting method is used in this paper, and the three-dimensional phase map restored using our method is shown in Fig. 1(c).

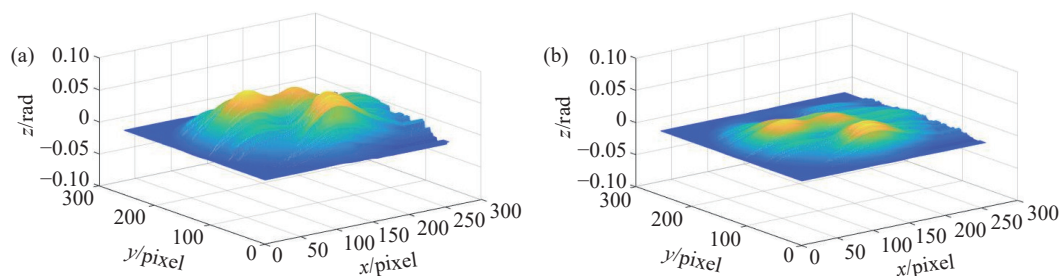
And the three-step phase-shifting method is adopted in this paper.

In the simulated nonlinear system, assuming $\gamma = 1.15$ in Eq. (1). We use a projector to project the simulated object and a CCD to capture the deformation fringes of the object. A series of processes, including Fourier transform, filtering, inverse Fourier transform, and the three-step phase-shifting method, are performed on the deformed fringes.

The phase error can be calculated after measuring the phase using the binary fringe defocusing method, the method of reference [1], the method of reference [10], and our method. The phase errors of the simulation results obtained by the above three methods are shown in Figs. 2(a)–(d), respectively.

The absolute average phase errors of Fig. 2(a), (b), (c), and (d) are 0.0226 rad, 0.0174 rad, 0.0115 rad, and 0.0078 rad, respectively. The value obtained by the method mentioned in this paper are 34.51% for Fig. 2(a), 44.83% for Fig. 2(b), and 67.83% for Fig. 2(c).

From the results in Fig. 2 and the absolute average of phase errors in the aforementioned figures, it is obvious that the phase error obtained using our method is relatively small.



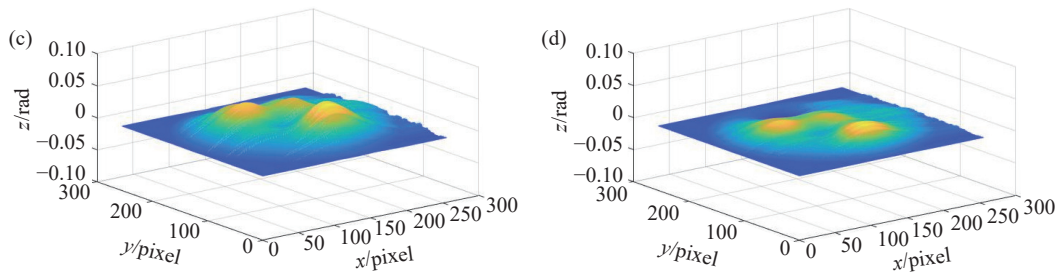


Fig. 2 Phase errors of recovered phase

3.2 Experiment

The actual experiments are now used to verify the correctness and reliability of the basic principle analysis proposed in this paper. The experimental process framework diagram is shown in Fig. 3.

An approximately cylindrical brim-shaped object is currently being used for the experiment. The phase diagram restored in the experiment using the three simulation methods above are shown in Figs. 4(a), (b), (c) and (d), respectively. The cross-

section of the recovered phase map of the 198th column is shown in Fig. 4(e).

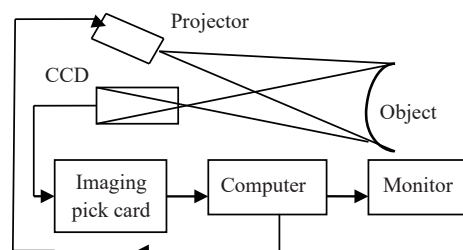


Fig. 3 The experimental process framework diagram

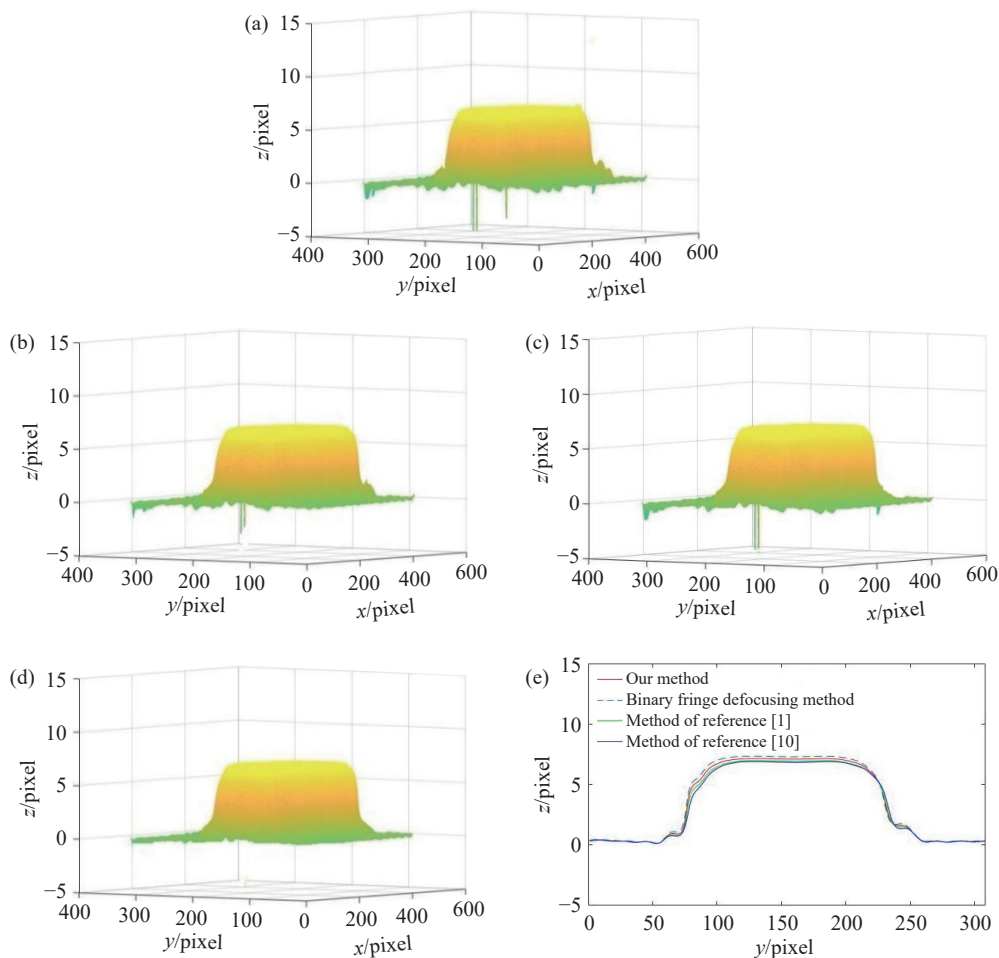


Fig. 4 The results of experiment

From the experimental results in Fig. 4, it is obvious that our method achieves good phase recovery results, with a correspondingly small phase error.

4 Conclusions

Due to nonlinear effects caused by optical measurement defocusing projection systems in practical situations, phase errors are generated during the measurement process. Therefore, the causes and reduction methods of phase errors in binary fringe defocusing projection have been analyzed and dis-

cussed in this paper, and a brief theoretical analysis and formula derivation of the basic principles have been provided.

Subsequently, the analysis and derivation of the basic principles were effectively validated through computer simulation and actual experimental verification. The comparative results indicate that the method mentioned in this paper can effectively filter out high-order harmonic components in the spectra domain and carry out phase unwrapping, resulting in better phase recovery and smaller phase errors.

References:

- [1] 乔闹生, 尚雪. 抽样对三维形貌测量的影响[J]. *中国光学*, 2024, 17(6): 1512-1520.
QIAO N SH, SHANG X. Influence of sampling on three-dimensional surface shape measurement[J]. *Chinese Optics*, 2024, 17(6): 1512-1520. (in Chinese).
- [2] GUO W B, WU ZH J, ZHANG Q C, *et al.*. Generalized phase shift deviation estimation method for accurate 3-D shape measurement in phase-shifting profilometry[J]. *IEEE Transactions on Instrumentation and Measurement*, 2025, 74: 5023511.
- [3] XIE Y, WANG X H, ZHOU Q. Phase calculation of smooth surface with multi-reflectivity based on phase measurement deflectometry[J]. *Optics Express*, 2024, 32(12): 20866-20880.
- [4] WANG L, ZHANG Y T, YI L N, *et al.*. Active projection nonlinear γ correction method for fringe projection profilometry[J]. *Journal of the Optical Society of America A*, 2022, 39(11): 1983-1991.
- [5] YANG SH CH, WEN J, WU SH W, *et al.*. Camera calibration with active standard Gaussian stripes for 3D measurement[J]. *Measurement*, 2024, 233: 114793.
- [6] 张正祺, 陈玉翀, 达飞鹏, 等. 基于双向条纹点云匹配的复杂纹理误差校正[J]. *中国光学(中英文)*, 2025, 18(5): 1086-1096.
ZHANG ZH Q, CHEN Y CH, DA F P, *et al.*. Error correction of complex texture objects based on bidirectional fringe projection point cloud matching[J]. *Chinese Optics*, 2025, 18(5): 1086-1096. (in Chinese).
- [7] 郭创为, 王阳, 邹文哲, 等. 基于多频外差原理的相位校正方法研究[J]. *红外与激光工程*, 2023, 52(5): 202206.
GUO CH W, WANG Y, ZOU W ZH, *et al.*. Study of phase correction method based on multi-frequency heterodyne principle[J]. *Infrared and Laser Engineering*, 2023, 52(5): 202206. (in Chinese).
- [8] LIU Y K, YU X, XUE J P, *et al.*. A flexible phase error compensation method based on probability distribution functions in phase measuring profilometry[J]. *Optics & Laser Technology*, 2020, 129: 106267.
- [9] WANG J, WU ZH X, HUANG Y Y, *et al.*. A rapid and accurate gamma compensation method based on double response curve fitting for high-quality fringe pattern generation[J]. *Optics & Laser Technology*, 2023, 160: 109084.
- [10] WANG J H, XU P, YANG Y X. Generic and flexible self-correction method for nonlinearity-induced phase error in three-dimensional imaging[J]. *Chinese Optics Letters*, 2024, 22(6): 061201.
- [11] ZHANG W, SHAN SH, LI Z, *et al.*. Correction of phase errors introduced by nonlinearity and specular reflection based on double N -step phase-shifting profilometry[J]. *Applied Physics B*, 2024, 130(1): 1.
- [12] TAN J, LIU J, WANG X, *et al.*. Large depth range binary-focusing projection 3D shape reconstruction via unpaired data learning[J]. *Optics and Lasers in Engineering*, 2024, 181: 108442.
- [13] SHEN S Y, LU R SH, LI H, *et al.*. High-speed 3D reconstruction with defocus composite fringes[J]. *Applied Optics*, 2024, 63(36): 9223-9231.

-
- [14] YUAN H S, ZENG H Y, WANG J, *et al.*. Superlarge depth range 3D measurement based on dual-focal optimization strategy[J]. *Optics Express*, 2025, 33(7): 16041-16051.
- [15] CAI Z W, LIU X L, JIANG H, *et al.*. Flexible phase error compensation based on Hilbert transform in phase shifting profilometry[J]. *Optics Express*, 2015, 23(19): 25171-25181.

Author Biography:



QIAO Nao-sheng (1971—), Ph.D, Professor, International College, Hunan University of Arts and Science. His research interests are optical information processing. E-mail: naoshengqiao@163.com